Magn Reson Med Sci 2019; 18; 36–43
doi:10.2463/mrms.mp.2017-0078
Published Online: March 23, 2018

MAJOR PAPER

The Reliability of Reduced Field-of-view DTI for Highly Accurate Quantitative Assessment of Cervical Spinal Cord Tracts

Takumi Yokohama[1*], Motoyuki Iwasaki[2], Daisuke Oura[1], Sho Furuya[2], and Tomoyuki Okuaki[3]

Purpose: To compare the accuracy of fractional anisotropy (FA) and apparent diffusion coefficient (ADC) values between reduced FOV or so-called zonally oblique multislice (ZOOM) and conventional diffusion tensor imaging (DTI) in the cervical spinal cord.

Methods: Both ZOOM and conventional DTI were performed on 10 healthy volunteers. Intraclass correlation coefficient (ICC) was used to evaluate the reliability of the measurements obtained. Four radiologists evaluated the FA and ADC values at each cervical cord level and classified the visibility by 4 ranks. The geometric distortion ratios of the long axis and short axis were compared between ZOOM and conventional DTI. The imaging parameters were as follows: *b*-value = 600 s/mm^2; TR = 4500 ms; TE = 81 ms; FOV = 70 × 47 mm^2 / 200 × 200 mm^2; matrix = 80 × 51 / 128 × 126 (ZOOM and conventional DTI, respectively). The region of interest was carefully drawn inside the spinal cord margin to exclude the spinal cord component, without excluding the white matter fiber tracts.

Results: The average FA value decreased in both ZOOM and conventional DTI in lower spinal cord levels; in contrast, the ADC value increased in lower spinal cord levels. Zonally oblique multislice DTI was superior to conventional DTI with regard to inter-rater and intra-rater reliability; further, visibility was better and the standard deviation was smaller in ZOOM DTI. On both the long and short axis, the geometric distortion ratio was lower in ZOOM DTI at all cervical spinal cord levels compared with the conventional DTI. There was a significant difference in the distortion ratios of the long and short axis between ZOOM and conventional DTI.

Conclusion: Conventional DTI is unreliable owing to its susceptibility to the surrounding magnetic field. ZOOM DTI is reliable for performing highly accurate evaluations.

Keywords: *fractional anisotropy, outer volume suppression, single-shot echo-planar imaging, small field-of-view*

Introduction

Diffusion-weighted imaging (DWI)[1] reflects the Brownian motion of water molecules, and it is widely used to diagnose brain infarction.[2] In addition, diffusion tensor imaging (DTI)[3] applied using the DWI technique can depict the structure of white matter fibers of the brain. Diffusion tensor imaging can calculate anisotropy of water molecules[4] as the fractional anisotropy (FA) value. Diffusion tensor imaging is expected to aid in predicting the outcome of patients with intracranial hematoma.[5] Recently, DTI was used for the quantitative evaluation of the spinal cord region.[6] Diffusion tensor imaging is generally acquired using single-shot echo-planar imaging (SS-EPI)[7] on a spin-echo (SE) sequence. The advantage of this technique is reduction of the ghost artifacts[8] caused by physiological motion of subjects. The *K*-space is filled with the combination of one excitation pulse and the inversion of a read-out gradient magnetic field on SS-EPI without the 180-degree refocus pulse used for conventional SE.[9] In general, magnetic artifacts occurring during DTI sequences are often observed on the cervical spinal cord owing to the surrounding unstable magnetic susceptibility region. Moreover, the cervical spinal cord is smaller than the whole brain. High-resolution images of cervical spinal cord DTI prolong the scan time, which is not preferable in a clinical setting. However, the lower resolution scan reduces the accuracy of the FA value. Considering such circumstances, a current technique such as zonally oblique multislice (ZOOM) DTI[10] was proposed.

Zonally oblique multislice DTI is based on a reduced FOV (rFOV)[11] with SS-EPI, which indicates that it is useful for

[1]Department of Radiology, Otaru General Hospital, 1-1-1 Wakamatsu, Otaru, Hokkaido 047-8550, Japan
[2]Department of Neurosurgery, Otaru General Hospital, Hokkaido, Japan
[3]Department of Radiology, Philips Healthcare, Tokyo, Japan
*Corresponding author, Phone: +81-34-25-1211, Fax: +81-34-32-6424, E-mail: takumi.c.rona@gmail.com

Received: June 5, 2017 | Accepted: February 7, 2018

obtaining diffused images in at least one-dimensionally limited area. Field-of-view reduction is achieved by the application of non-coplanar excitation and refocusing pulses combined with outer volume suppression (OVS) for removal of unwanted transition zones.[12] The outline of ZOOM DTI is shown in Fig. 1. Zonally oblique multislice DTI is based on a non-coplanar SE technique,[13] which apply tilted radio frequency (RF) pulse between the excitation and the slice-selective region. As a result, a small, limited region is excited. Furthermore, the suppression pulse is imposed around the FOV, which is excited by non-coplanar SE to establish a rectangular FOV. This technique is called OVS.[13] Small, non-distortion FOV is acquired by non-coplanar SE and OVS on ZOOM DTI. A diagram of ZOOM DTI is shown in Fig. 2. Zonally oblique multislice DTI is a diffusion-weighted (DW) SS-EPI sequence, and it is preceded by presaturation OVS sequence and the spectral presaturation with inversion recovery pulse. Suppression slabs are implemented by successive quadratic phase RF pulses[14] (broad bandwidth, selective) followed by crusher gradients, and a small, non-distortion FOV image can be acquired by this technique. The advantages of cervical spinal DTI with ZOOM DTI are as follows: small FOV imaging reduces the readout scan time, so the artifact caused by off-resonance is also decreased.[12] The phase encode step is reduced and no phase wrap is required owing to the limited FOV excited with non-coplanar SE and OVS.[15] Hence, a fine cervical spinal cord DTI is obtained after a short scan time using ZOOM DTI.[10] However, the differences in the reliability of the FA and ADC value measurements between ZOOM and conventional DTI have not been determined. The purpose of this study was to compare and establish the reliability of measured FA and ADC values and image quality using ZOOM DTI compared with conventional-DTI for the cervical spinal cord.

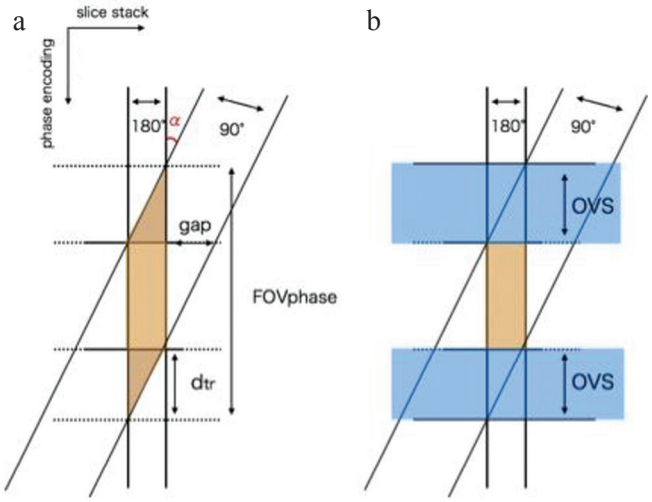

Fig. 1 Non-coplanar spin-echo (SE). (**a**) In general, the 90° radio frequency (RF) pulse is applied perpendicular to the imaging plane, but the 90° RF pulse is applied tilted by a small angle, α, with respect to the imaging plane. This approach allows multiple-slice acquisition, but achieves an imperfect signal profile with an unwanted transition width d_{tr}. (**b**) The 90° RF pulse is again tilted by angle α, but additional outer volume suppression slabs are applied on both sides. OVS, outer volume suppression.

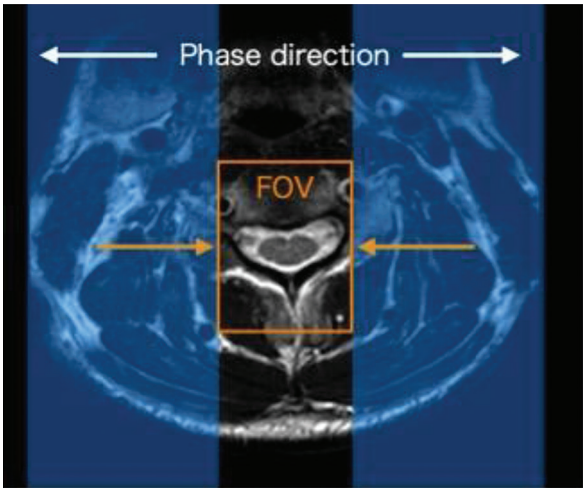

Fig. 2 The location of outer volume suppression (OVS). The OVS is located, although no folding occurs in the phase direction.

Materials and Methods

Device and imaging target

Imaging was performed on 10 healthy volunteers (mean age, 31.9 years [range, 23–57 years], 6 men and 4 women), using a 3T MR scanner (Ingenia; Koninklijke Philips N.V., Amsterdam, Netherlands). This study was approved by the Institutional Review Board of Otaru General Hospital.

Imaging parameters

Zonally oblique multislice and conventional DTI imaging sequences were used to obtain cervical spinal DTI images. Imaging settings are shown in Table 1.

Zonally oblique multislice DTI parameters were as follows: TR = 4500 ms; TE = 81 ms; FOV = 70 × 47 mm^2;

Table 1 Sequence parameters for performance of cervical spine diffusion tensor imaging (DTI) using ZOOM and conventional DTI

Sequence	ZOOM DTI	Conventional DTI
TR (ms)	4500	4500
TE (ms)	81	81
Matrix size (phase × read out)	72 × 46	128 × 126
FOV (mm)	70 × 47	200 × 200
Slice thickness (mm)	5	5
Slices	24	24
NSA	10	5
b-factor (s/mm^2)	600	600
Fat suppression	SPAIR	SPAIR
Scan time	10 min 35 sec	10 min 3 sec

NSA, number of sample averages; SPAIR, spectral attenuated inversion recovery; ZOOM, zonally oblique multislice.

matrix = 80 × 51; number of sample averages (NSA) = 10; scan time = 10 min 35 sec. Conventional DTI parameters were as follows: TR = 4500 ms; TE = 81 ms; FOV = 200 × 200 mm^2; matrix = 128 × 126; NSA = 5; scan time = 10 min 3 sec.

Scan time was set to the same interval in both settings, and the following parameters were the same: single-shot SE, *b*-value 600 s/mm^2; 6 motion probing gradient (MPG) direction; slice thickness of 5 mm; and 24 slices. The acquired scan range was from the second cervical to the first thoracic vertebra. The slab center was placed at C4/5. The range of imaging for ZOOM and conventional DTI is shown in Fig. 3.

Evaluation and analysis

Quantitative value by cervical spine level

The FA map was calculated on ZOOM and conventional DTI. The FA value and apparent diffusion coefficient (ADC) of the spinal cord were measured. The ROI was placed on the spinal cord and enlarged maximally; however, the surrounding cerebrospinal fluid (CSF) was excluded by checking the 3D ROI square. The method used for setting the ROI is shown in Fig. 4. All operations were performed using Fiber Track (Philips Electronics Japan, Tokyo, Japan), the software in the MRI scanner. The mean and standard deviation (SD) of the FA value was calculated using scan data of 10 healthy volunteers. The Wilcoxon rank sum test was used for statistical analysis; analyses were performed using JMP version 12 (SAS Institute, Inc., Cary, NC, USA).

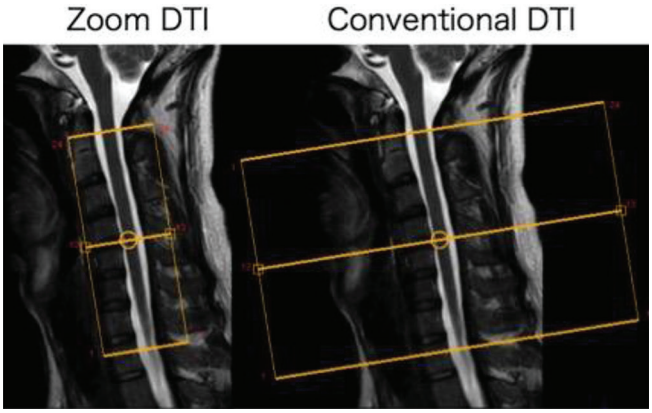

Fig. 3 The imaging range of zonally oblique multislice (ZOOM) diffusion tensor imaging (DTI) and conventional DTI.

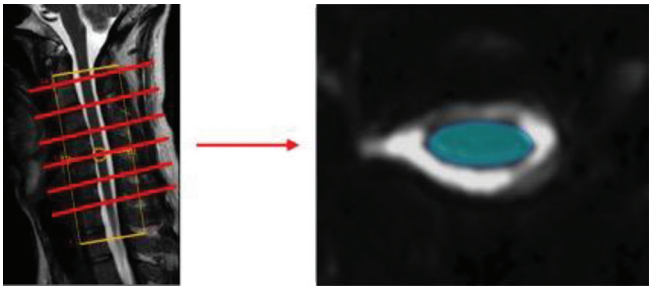

Fig. 4 Setting of the ROI for the cervical spinal cord. Notably, the entire cord was contoured as widely as possible while excluding the surrounding cerebrospinal fluid.

Evaluation of measurements

To examine the reliability of the measurements obtained from spinal cord imaging in 10 volunteers, intraclass correlation coefficient (ICC)[16] was used to evaluate the inter-rater and intra-rater reliability of the FA and the ADC values. According to Shrout et al., ICC has three forms, namely Case 1, Case 2, and Case 3 (thesis) and can be expressed as ICC (*n*, *k*), where *n* refers to Case 1, 2, or 3, and *k* indicates number of people.

Intraclass correlation coefficient Case 1 is the intra-examiner confidence factor when one observer evaluates multiple subjects, and it is calculated by the following equation:

$$\mathrm{ICC}\ (1,1) = \frac{\mathrm{BMS} - \mathrm{WMS}}{\mathrm{BMS} + (k-1)\ \mathrm{WMS}}$$

$$\mathrm{ICC}\ (1,k) = \frac{\mathrm{BMS} - \mathrm{WMS}}{\mathrm{BMS}}$$

where BMS is between sum of mean square, WMS is within sum of mean square.

The difference between Case 2 and Case 3 is that the former is a random effect model and the latter is a fixed model. In this study, we adopted Case 2, which was calculated by the following formula:

$$\mathrm{ICC}\ (2,1) = \frac{\mathrm{BMS} - \mathrm{EMS}}{\mathrm{BMS} + (k-1)\ \mathrm{EMS} + k\ (\mathrm{JMS} - \mathrm{EMS})\ /\ n}$$

where EMS is the residual sum of mean square, and JMS is the judges sum of mean square.

The inter-rater reliability was evaluated by three radiologists (years of experience: 12, 5, and 3 years). The criteria of ICC are shown in Table 2.

Image quality

We compared the image qualities of ZOOM and conventional DTI using a 4-point scale visual evaluation. Four radiological technologists with 26, 14, 11, and 2 years of experience evaluated the distortion with *b* = 0 image as the visibility. Transverse images of each cervical spinal cord level evaluated are shown in Fig. 5. The scoring system was as follows: 4 = no image distortion, and spinal cord and CSF can be clearly discriminated; 3 = minimal image distortion, and the cord-CSF boundary line can be discriminated; 2 = considerable image

Table 2 The criteria of intraclass correlation coefficient (ICC)

0.9	Great
0.8	Good
0.7	Ok (fair)
0.6	Possible
0.6	Re-work

Re-work is necessary for ICC less than 0.6.

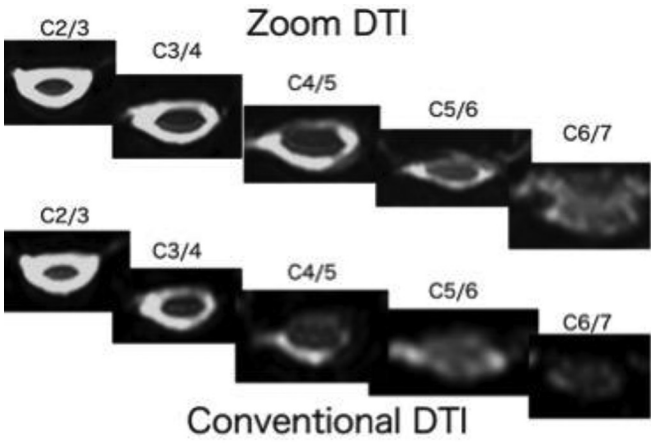

Fig. 5 A comparison of axial images of the cervical spinal cord highlights the remarkable difference in visibility when defining the ROI.

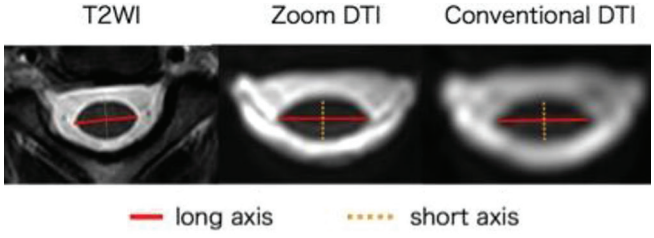

Fig. 6 Measurement of the distortion ratio using the National Electrical Manufacturers Association method. The lengths of the long and short axis were measured, and geometric distortion ratio was measured from the ratio with the reference value.

distortion, and it is difficult to discriminate the cord-CSF boundary line; 1 = poor image quality, and a cord-CSF boundary that cannot be completely differentiated.

Data were analyzed using the Tukey–Kramer method; a P-value < 0.05 was considered significant.

The distortion evaluation using the NEMA method

On a $b = 0$ image, we compared the geometric distortion ratio of the long and short axis between ZOOM DTI and conventional DTI by the National Electrical Manufacturers Association (NEMA) method.[17] A transverse T_2-weighted image (T_2WI) obtained using a fast SE sequence was used as a standard image. Measurement of the long and short axis is shown in Fig. 6. The geometric distortion ratio was calculated using the following equation:

$$\text{Geometric distortion ratio} = (\text{Lm} - \text{La}) / \text{La} \times 100$$

where Lm = the length of the standard image and La = the length of the DTI image. Data were analyzed using the Wilcoxon rank sum test; a P-value < 0.05 was considered significant.

Measurement of SNR

The signal-to-noise ratio (SNR) for spinal cord imaging using the ZOOM and conventional DTI was calculated using ImageJ (National Institutes of Health, Bethesda, MD, USA), and the average value was obtained.

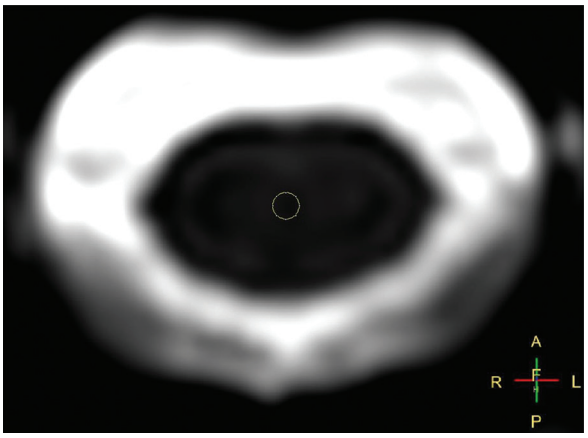

Fig. 7 The measurement of signal-to-noise ratio. The size of the ROI was a circle with a diameter of 30 mm, so that it does not contain the cerebrospinal fluid component.

The ROI was a circle with a diameter of 30 mm and did not contain the CSF component. The setting of the ROI is shown in Fig. 7. The SNR can be obtained by the following equation:

$$\text{SNR} = \frac{\text{Signal intensity (SI)}}{\text{Standard devitation (SD)}}$$

Results

Quantitative values of the cervical spine

Fractional anisotropy and ADC values obtained using ZOOM and conventional DTI are shown in Table 3 and Figs. 8–11. The FA and ADC values of the cervical spinal cords were approximately 0.6 and 1.0, respectively. In both ZOOM and conventional DTI, the average FA value decreased in lower spinal cord levels; in contrast, the ADC value increased in lower spinal cord levels. The SD of the FA and ADC values were significantly higher in the lower cervical spine, especially at C5/6 and C6/7, in the conventional DTI compared with ZOOM DTI.

Reliability of the measurements

The intra- and inter-rater reliability at each cervical spinal cord level is shown in Tables 4 and 5. In terms of inter-rater reliability, for the FA value, ICC (2, 1) for ZOOM DTI was higher than 0.7 in all cervical spinal cords; however, in conventional DTI, ICC (2, 1) was less than 0.6 at C5/6. Similarly, for the ADC value, ICC (2, 1) for ZOOM DTI was larger than 0.6 in all the cervical spinal cords; in contrast, for the conventional DTI, ICC (2, 1) was less than 0.6 at C2/3, C4/5, and C5/6.

In terms of intra-rater reliability, for the FA value, ICC (1, 1) was higher than 0.6 in all cervical spinal cords in both ZOOM and conventional DTI. By contrast, for the ADC value, ICC (1, 1) for ZOOM DTI was less than 0.6 at C2/3.

Table 3 Mean and standard deviation of fractional anisotropy (FA) and apparent diffusion coefficient (ADC) at each cervical spinal level

	FA			ADC		
	ZOOM DTI (n = 10)	Conventional DTI (n = 10)	P value*	ZOOM DTI (n = 10)	Conventional DTI (n = 10)	P value*
C2/3	0.717 ± 0.0576	0.681 ± 0.0543	0.1303	0.9893 ± 0.1031	1.026 ± 0.9707	0.4497
C3/4	0.690 ± 0.0613	0.684 ± 0.0858	0.5967	0.9610 ± 0.1013	1.027 ± 0.2040	0.5706
C4/5	0.636 ± 0.0742	0.629 ± 0.123	0.7624	1.052 ± 0.2033	1.125 ± 0.3263	0.8798
C5/6	0.594 ± 0.0698	0.632 ± 0.0879	0.1509	1.163 ± 0.1857	1.140 ± 0.2068	0.7335
C6/7	0.554 ± 0.0854	0.569 ± 0.00804	0.7624	1.294 ± 0.1956	1.251 ± 0.2603	0.7054

*Wilcoxon rank sum test; values are presented as means ± standard deviations in a ROI. DTI, diffusion tensor imaging; ZOOM, zonally oblique multislice.

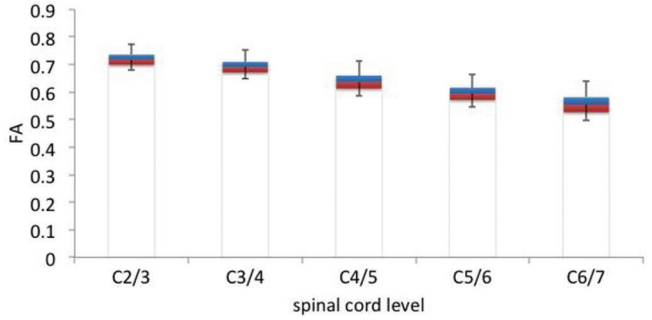

Fig. 8 Fractional anisotropy (FA) value at each cervical spinal level in zonally oblique multislice (ZOOM) diffusion tensor imaging. The FA value gradually decreased at the lower spinal cord levels.

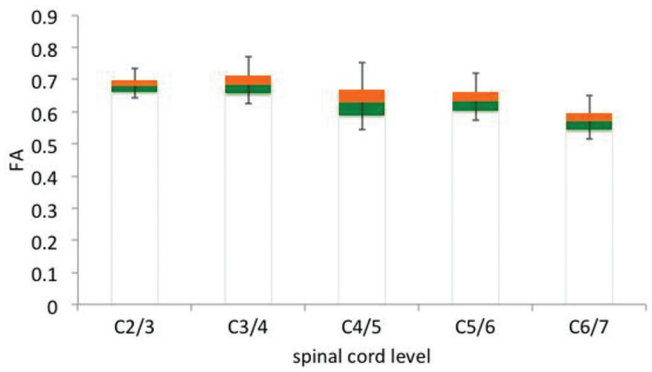

Fig. 9 Fractional anisotropy (FA) value at each cervical spinal level in conventional diffusion tensor imaging (DTI). Note that the lower levels show a wider range of value than zonally oblique multislice (ZOOM) DTI.

Additionally, ICC (1, 1) for conventional DTI was less than 0.6 at C2/3 and C6/7.

Image quality

The result of an image quality evaluation is displayed in Fig. 12. Zonally oblique multislice DTI was superior to conventional DTI at all cervical spinal levels using a 4-point scoring system. The scores at all cervical levels in ZOOM DTI were significantly higher than those of the conventional DTI.

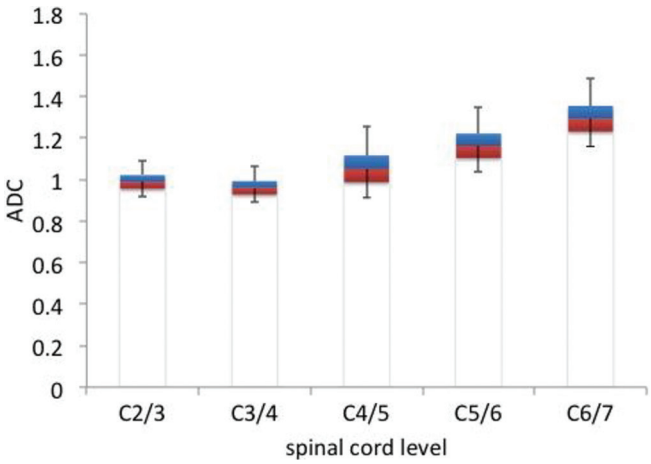

Fig. 10 Apparent diffusion coefficient (ADC) value at each cervical spinal level on zonally oblique multislice (ZOOM) diffusion tensor imaging.

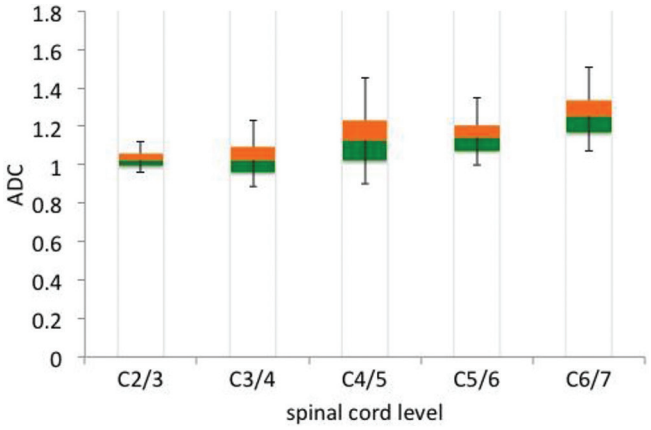

Fig. 11 Apparent diffusion coefficient (ADC) value at each cervical spinal level on conventional diffusion tensor imaging.

Distortion evaluation using the NEMA method

The results of the geometric distortion ratio are shown in Table 6 and Figs. 13 and 14. On both the long and short axis, the geometric distortion ratio was lower in ZOOM DTI at all cervical spinal cord levels compared with the conventional

Table 4 Inter-rater reliability between ZOOM and conventional DTI

	FA		ADC	
	ZOOM	Conventional	ZOOM	Conventional
C2/3	0.881	0.788	0.648	0.207
C3/4	0.721	0.620	0.602	0.686
C4/5	0.839	0.637	0.684	0.543
C5/6	0.818	0.140	0.601	0.251
C6/7	0.877	0.769	0.628	0.733

Intraclass correlation coefficient (2, 1) was performed; values are calculated from variance analysis. DTI, diffusion tensor imaging; FA, fractional anisotropy; ADC, apparent diffusion coefficient; ZOOM, zonally oblique multislice.

Table 5 Intra-rater reliability between ZOOM and conventional DTI

	FA				ADC			
	ZOOM		Conventional		ZOOM		Conventional	
	ICC (1, 1)	ICC (1, 3)	ICC (1, 1)	ICC (1, 3)	ICC (1, 1)	ICC (1, 3)	ICC (1, 1)	ICC (1, 3)
C2/3	0.960	0.986	0.821	0.932	0.612	0.825	0.570	0.799
C3/4	0.618	0.963	0.915	0.970	0.848	0.943	0.754	0.902
C4/5	0.949	0.982	0.970	0.990	0.793	0.920	0.971	0.990
C5/6	0.942	0.980	0.922	0.973	0.787	0.917	0.753	0.901
C6/7	0.724	0.887	0.677	0.863	0.277	0.534	0.585	0.809

ICC (1, 1) and ICC (1, 3) were performed; values are calculated from variance analysis. ICC, Intraclass correlation coefficient; FA, fractional anisotropy; ADC, apparent diffusion coefficient; ZOOM, zonally oblique multislice.

DTI. The geometric distortion ratio was higher on the short axis than in the long axis.

There was a significant difference in the distortion ratio of the long axis between ZOOM and conventional DTI at each spinal cord level; C2/3: 1.216% and 7.672% ($P < 0.05$); C3/4: 1.396% and 9.098% ($P < 0.01$); C4/5: 2.283% and 10.44% ($P < 0.05$); and C5/6: 8.347% and 21.55% ($P < 0.05$), in ZOOM and conventional DTI, respectively. Similarly, the distortion ratio of the short axis was significantly different at C3/4: 0.3231% and 19.11% ($P < 0.01$), in ZOOM DTI and conventional DTI, respectively.

Signal-to-noise ratio

The results of SNR obtained at each spinal cord level are shown in Table 7 and Fig. 15. Although ZOOM DTI showed a larger variation in SNR, its SNR was larger than that of conventional DTI, except at C4/5.

Discussion

In this study, the acquired FA and ADC values at each cervical spinal level were approximately 0.6 and 1.0, respectively. The FA and ADC value were equivalent when compared with previous studies.[18,19] However, we obtained a stable FA and ADC value in ZOOM DTI with regard to their SD at each

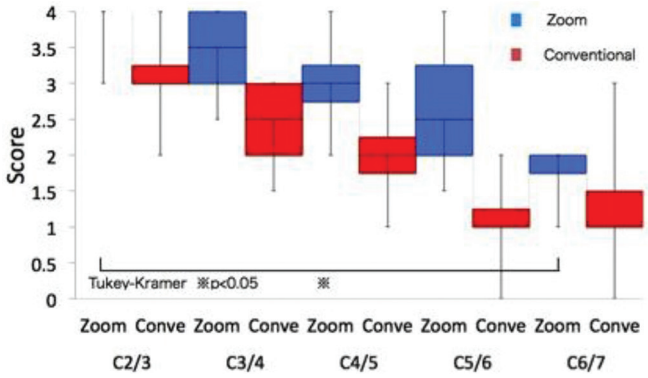

Fig. 12 Visual assessment of cervical spinal cord using 4-point scoring. ZOOM, zonally oblique multislice DTI; Conve, conventional DTI; DTI, diffusion tensor imaging.

Table 6 Geometric distortion of the long and short axis of ZOOM and conventional DTI evaluated by the NEMA method

	Geometric distortion (%)					
	Long axis			Short axis		
	ZOOM DTI	Conventional DTI	*P*-value*	ZOOM DTI	Conventional DTI	*P* value*
C2/3	1.216	7.672	0.0046	11.20	26.36	0.1509
C3/4	1.396	9.098	0.0007	0.3231	19.11	0.0041
C4/5	2.283	10.44	0.0189	10.26	25.68	0.0962
C5/6	8.347	21.55	0.0126	30.87	53.57	0.4507
C6/7	9.964	16.84	0.1736	41.69	58.17	0.3845

*Wilcoxon rank sum test; Values are geometric distortion. DTI, diffusion tensor imaging; NEMA, National Electrical Manufacturers Association; ZOOM, zonally oblique multislice.

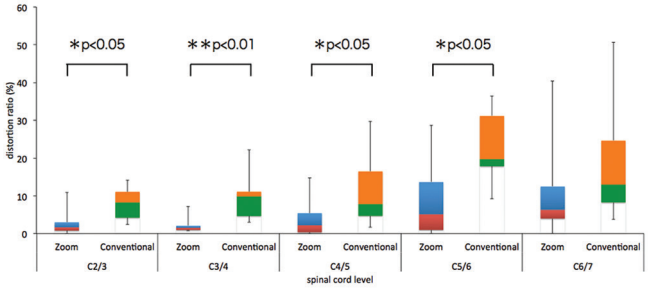

Fig. 13 Distortion ratio of the long axis. ZOOM, zonally oblique multislice.

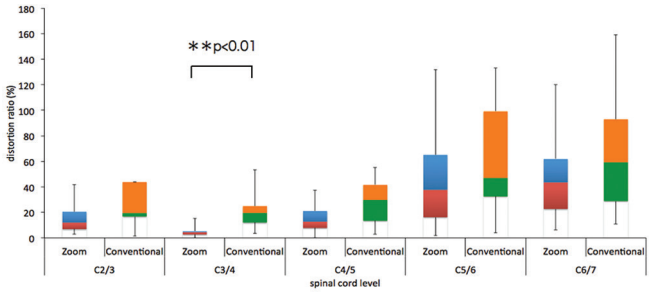

Fig. 14 Distortion ratio of the short axis. ZOOM, zonally oblique multislice.

spinal level. High accuracy of the estimated value is desired for the quantitative analysis of DTI when we assess the fiber tracts. However, quantitative values, which depend on the examiner, have poor repeatability. In our study, ICC (2, 1) of the FA and ADC values obtained for ZOOM DTI was higher than 0.6 in all cervical spinal cord levels compared to that for conventional DTI; this suggests the stability of the measurements. Additionally, for intra-rater reliability, it is considered that a more accurate quantitative value can be obtained by increasing the number of measurements taken.

Variable artifacts often occur on neck MRIs.[20] In particular, these artifacts are evident at lower spinal levels (C5–Th1). These are mainly derived from magnetic susceptibility and motion during imaging. Magnetic susceptibility artifacts are caused by magnetic field nonuniformity due to air in the lung apex and surrounding the complex figure of the neck level. Motion artifacts also result from swallowing movements. These effects also reflect the result of the distortion ratio. In echo planar sequences such as DTI, the distortion generally occurs in the phase encode direction. Therefore, the geometrical distortion ratio of the short axis was higher than that of the long axis. Further, the difference in distortion between ZOOM and conventional DTI was smaller at the lower spinal cord levels.

In other words, despite ZOOM DTI being an EPI sequence, its rFOV, based on non-coplanar SE and OVS, can be useful in obtaining images with less distortion and higher accuracy.

In ZOOM DTI, it is difficult to distinguish between white matter and gray matter at sites that show high distortion such as the lower cervical spinal cord; however, they can be distinguished in the upper cervical spinal cord.

Zonally oblique multislice DTI showed a higher SNR compared to conventional DTI, but conventional DTI uses the sensitivity encoding (SENSE) technique, which seems to cause the increase in noise.

Additionally, the variation in SNR is larger in ZOOM DTI; this is attributed to the influence of breathing and body shape of the subjects.

We compared the image quality of DTI between the two techniques and determined that the visibility with ZOOM DTI was superior to that with conventional DTI. Notably, image quality was lower at a lower cervical level in both techniques. In particular, scores of conventional DTI at C5/6 and 6/7 were remarkably lower. There was a significant difference between C2/3 and C6/7 on ZOOM DTI.

Non-coplanar SE and OVS would help to overcome the limitations of ZOOM DTI despite the EPI sequences. Spatial resolutions of DTI images would be important for accurate measurements. A previous report mentioned that misleading results were caused by the partial volume effect between white matter and CSF.[21] In particular, in a small organ such as the spinal cord, fine resolution that can depict a clear boundary between the subject and the surrounding tissue would be preferable. Of note, fluctuation in FA and ADC values was strongly influenced by CSF. Therefore, contouring of the ROI is very important to obtain highly accurate quantitative values. Region of interest should be set strictly inside the spinal cord and enlarged maximally, while excluding the possibility of encasement of CSF by checking 3D ROI squares. In this study, reduction of the FA value at the C6/7 level implies the difficulty of excluding the CSF influence when setting the ROI around the apex of the cervical cord sagittal curvature. Cerebrospinal fluid involvement, susceptibility, and motion artifacts at lower levels, especially in C5/6 and 6/7, cannot be ignored even in ZOOM DTI. However, SE imaging ordinarily reduces susceptibility and motion artifacts compared to EPI, so ZOOM DTI was superior for acquisition of less distorted DTI than the conventional method. Recently, new DTI imaging modalities based on turbo SE were developed.[22] This technique can potentially reduce susceptibility artifacts and distortion at the lower level of the spinal cord. The in-plane resolution of ZOOM DTI was 1 mm^2, whereas that of conventional DTI was 1.56 mm^2 for a similar scan time. Zonally oblique multislice DTI did not require phase over-sampling such as no-phase warp to establish a small FOV. High-resolution assessment within the available scan time in a clinical setting could be achieved by ZOOM DTI. In future studies, a time reduction technique, such as multi-band SENSE[23] may contribute to the shorter scan time of DTI.

Table 7 Mean and standard deviation of signal-to-noise ratio (SNR) at each cervical spinal cord level

	Zoom	Conventional	*P* value*
C2/3	21.07 ± 13.98	15.81 ± 5.896	0.6501
C3/4	29.42 ± 24.90	18.97 ± 7.152	1
C4/5	17.39 ± 17.43	19.89 ± 11.48	0.1306
C5/6	31.45 ± 24.09	15.75 ± 6.873	0.2899
C6/7	26.32 ± 22.55	17.04 ± 13.08	0.3643

*Wilcoxon rank sum test; values are presented as means ± standard deviations in a ROI. ZOOM, zonally oblique multislice.

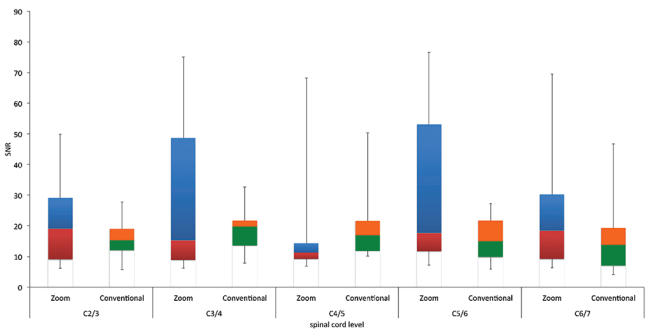

Fig. 15 Signal-to-noise ratio (SNR) of zonally oblique multislice (ZOOM) and conventional diffusion tensor imaging in 10 healthy volunteers.

Conclusions

This study revealed the advantage of ZOOM. DTI for the quantitative estimation of cervical spinal cord tracts. Zonally

oblique multislice DTI provides better visibility and high accuracy using a small FOV and a shorter practical scan time compared with conventional DTI. The ROI contour should not include the surrounding CSF; however, susceptibility and motion artifacts at lower cervical levels cannot be completely avoided even in ZOOM DTI. To attain further rapid, high-resolution DTI sequences, combined ZOOM DTI and recently introduced techniques such as turbo spin-echo (TSE)-DWI and multi-band SENSE are desirable.

Acknowledgments

The authors would like to thank Philips Healthcare for supporting this study. They also would like to thank Editage (www.editage.jp) for English language editing.

Conflicts of Interest

Tomoyuki Okuaki is an employee of Philips Healthcare. The other authors declare that they have no conflicts of interest.

References

1. Hagmann P, Jonasson L, Maeder P, Thiran JP, Wedeen VJ, Meuli R. Understanding diffusion MR imaging techniques: from scalar diffusion-weighted imaging to diffusion tensor imaging and beyond. Radiographics 2006; 26:S205–S223.
2. van Everdingen KJ, van der Grond J, Kappelle LJ, Ramos LM, Mali WP. Diffusion-weighted magnetic resonance imaging in acute stroke. Stroke 1998; 29:1783–1790.
3. Basser PJ, Mattiello J, LeBihan D. MR diffusion tensor spectroscopy and imaging. Biophys J 1994; 66:259–267.
4. Mukherjee P, Berman JI, Chung SW, Hess CP, Henry RG. Diffusion tensor MR imaging and fiber tractography: theoretic underpinnings. AJNR Am J Neuroradiol 2008; 29:632–641.
5. Kim JH, Kwon YM, Son SM. Motor function outcomes of pediatric patients with hemiplegic cerebral palsy after rehabilitation treatment: a diffusion tensor imaging study. Neural Regen Res 2015; 10:624–630.
6. Kitamura M, Eguchi Y, Inoue G, et al. A case of symptomatic extra-foraminal lumbosacral stenosis ("far-out syndrome") diagnosed by diffusion tensor imaging. Spine 2012; 37:E854–E857.
7. Mukherjee P, Chung SW, Berman JI, Hess CP, Henry RG. Diffusion tensor MR imaging and fiber tractography: technical considerations. AJNR Am J Neuroradiol. 2008; 29:843–852.
8. Skare S, Newbould RD, Clayton DB, Albers GW, Nagle S, Bammer R. Clinical multishot DW-EPI through parallel imaging with considerations of susceptibility, motion, and noise. Magn Reson Med 2007; 57:881–890.
9. Thian YL, Xie W, Porter DA, Weileng Ang B. Readout-segmented echo-planar imaging for diffusion-weighted imaging in the pelvis at 3T-A feasibility study. Acad Radiol 2014; 21:531–537.
10. Wilm BJ, Svensson J, Henning A, Pruessmann KP, Boesiger B, Kollias SS. Reduced field-of-view MRI using outer volume suppression for spinal cord diffusion imaging. Magn Reson Med 2007; 57:625–630.
11. Saritas EU, Cunningham CH, Lee JH, Han ET, Nishimura DG. DWI of the spinal cord with reduced FOV single-shot EPI. Magn Reson Med 2008; 60:468–473.
12. Zaharchuk G, Saritas EU, Andre JB, et al. Reduced field-of-view diffusion imaging of the human spinal cord: comparison with conventional single-shot echo-planar imaging. AJNR Am J Neuroradiol 2011; 32:813–820.
13. Wilm BJ, Gamper U, Henning A, Pruessmann KP, Kollias SS, Boesiger P. Diffusion-weighted imaging of the entire spinal cord. NMR Biomed 2009; 22:174–181.
14. Schulte RF, Tsao J, Boesiger P, Pruessmann KP. Equi-ripple design of quadratic-phase RF pulses. J Magn Reson 2004; 166:111–122.
15. Saritas EU, Cunningham CH, Lee JH, Han ET, Nishimura DG. DWI of the spinal cord with reduced FOV single-shot EPI. Magn Reson Med 2008; 60:468–473.
16. Shrout PE, Fleiss JL. Intraclass correlations: uses in assessing rater reliability. Psychol Bull 1979; 86:420–428.
17. National Electrical Manufactures Association. Determination of two-dimensional geometric distortion in diagnostic magnetic resonance images. NEMA Standards Publication. MS2-2008 (R2014) 2015.
18. Dowell NG, Jenkins TM, Ciccarelli O, Miller DH, Wheeler-Kingshott CA. Contiguous-slice zonally oblique multislice (CO-ZOOM) diffusion tensor imaging: examples of in vivo spinal cord and optic nerve applications. J Magn Reson Imaging 2009; 29:454–460.
19. Budrewicz S, Szewczyk P, Bladowska J, et al. The possible meaning of fractional anisotropy measurement of the cervical spinal cord in correct diagnosis of amyotrophic lateral sclerosis. Neurol Sci 2016; 37:417–421.
20. Krupa K, Bekiesińska-Figatowska M. Artifacts in magnetic resonance imaging. Pol J Radiol 2015; 80:93–106.
21. Roine T, Jeurissen B, Perrone D, et al. Isotropic non-white matter partial volume effects in constrained spherical deconvolution. Front Neuroinform 2014; 8:28.
22. Aggarwal M, Mori S, Shimogori T, Blackshaw S, Zhang J. Three-dimensional diffusion tensor microimaging for anatomical characterization of the mouse brain. Magn Reson Med 2010; 64:249–261.
23. Preibisch C, Castrillón G JG, Bührer M, Riedl V. Evaluation of multiband EPI acquisitions for resting state fMRI. PLoS ONE 2015; 10:e0136961.